

HiSST: 4th International Conference on High-Speed Vehicle Science Technology

22 -26 September 2025, Tours, France



Induced Transition to Turbulence in a Hypersonic Flow Over a Two-Dimensional Wedge

Talluri Vamsi Krishna¹, Jacob Cohen², S.K. Karthick³ and Soumya R. Nanda⁴

Abstract

The transition of boundary layers in hypersonic flows plays a decisive role in the design of thermal protection systems and the overall integrity of high-speed vehicles. This study investigates the influence of cylindrical surface roughness on the laminar–turbulent transition within a hypersonic boundary layer. Experiments were conducted in a Ludwieg tube facility using a wedge model fitted with cylindrical roughness elements of varying relative heights, corresponding to height-to-boundary-layer-thickness ratios (h/ δ) of 0.46, 0.77, and 1.15. Flow evolution downstream of the roughness was examined through high-speed Schlieren imaging and Planar Laser Rayleigh Scattering (PLRS), while unsteady pressure sensors embedded in the surface provided quantitative measurements of pressure fluctuations. The findings show that larger roughness elements significantly advance the transition location. The tallest trip (h/ δ = 1.15) produced substantial boundary layer thickening and the formation of vortical structures characteristic of turbulence. Pressure measurements revealed elevated root-mean-square (RMS) levels due to the transition. Furthermore, Proper Orthogonal Decomposition (POD) of spanwise PLRS data confirmed the emergence of coherent vortical structures downstream of x/D > 3.5 for the higher trip cases.

Keywords: Laminar to Turbulent Transition, Hypersonic, Roughness,

Nomenclature

D – Diameter of roughness element

f – frequency

h – height of roughness element

M – Mach Number

p – pressure

Re – Reynolds Number

x – Downstream distance from roughness

element

 δ – boundary layer thickness

1. Introduction

Laminar-to-turbulent transition in hypersonic boundary layers is critical for aerodynamic vehicles' performance, safety, and thermal protection. It significantly impacts heat transfer, drag, and structural integrity, with turbulence increasing surface heat flux and thermal stresses. Despite its importance, transition mechanisms are not yet fully understood, driven by Gortler, Mack's modes [1], and crossflow [2] instabilities. Accurate prediction is essential for optimizing high-speed vehicle design and reliability. Over the last five decades, extensive transition experiments have been conducted in traditional ground-testing facilities [3] using cones [4], flat plates, and wedges. These studies, including natural and induced transition [5], aim to understand the transition behavior and identify sources of unsteadiness. Nevertheless, even the laminar-to-turbulent induced transition process is still not fully understood. In particular, the origin of flow unsteadiness and its connection to first and second-mode instabilities, especially for cases where the trip height is smaller or larger than the boundary-layer thickness, are not fully explored.

¹Technion-Israel Institute of Technology, Haifa, Israel, Email: sri.vamsi1432@gmail.com

² Technion-Israel Institute of Technology, Haifa, Israel, Email: aerycyc@technion.ac.il

³ Indian Institute of Technology Kanpur, India Email: skkarthick@mae.iith.ac.in

⁴ Indian Institute of Technology Kanpur, India Email: srnanda@iitk.ac.in

In this context, detailed experiments are designed to examine the influence of the geometric parameter of the roughness element on the laminar—turbulent transition across a wide range of Reynolds numbers. Qualitative assessments are carried out using high-speed Schlieren imaging in conjunction with spanwise Planar Laser Rayleigh Scattering (PLRS). In addition, quantitative analysis is focused on the characterization of the fluctuating pressure distributions downstream of the cylinder location.

2. Experimental Setup

The experiments were conducted at a Mach 6 over a two-dimensional wedge using a 15° wedge model, corresponding to a Mach number over the wedge of 4.0. The tests were performed in the Hypersonic Ludwieg Tunnel (HLT) at the Technion wind tunnel complex, which can generate a hypersonic flow at Mach 6 for 12.5 milliseconds [6]. Figure 1 presents a model schematic, indicating the sensors' locations and the cylindrical roughness position. To trigger transition, cylindrical roughness elements with a diameter (D) of 5 mm and heights of 0.3, 0.5 and 0.75 mm were used. Table 1 presents the freestream conditions generated over the wedge for different Reynolds numbers. The thickness of the boundary layer was estimated using image analysis based on Schlieren visualization, measuring approximately 0.65 mm at the location of the cylindrical protuberance (37 mm downstream of the leading edge). Based on this, the height-to boundary-layer thickness ratios are $h/\delta = 0.46$, 0.77 (within the boundary layer) and $h/\delta = 1.15$ (above), respectively. To investigate the transition process, qualitative measurements were obtained through high-speed Schlieren imaging and spanwise Planar Laser Rayleigh Scattering (PLRS). In parallel, quantitative data were collected by measuring mean and fluctuating pressure distributions downstream of the cylinder. Flow visualization was carried out using two high-speed cameras: Schlieren imaging with a Phantom V1310 and PLRS imaging with a Fast Cam Nova S16. The PLRS system recorded high-resolution images at 768 × 560 pixels with a sampling rate of 60 kHz, while the Schlieren system captured images at 128×64 pixels with a higher sampling rate of 550 kHz. For pressure measurements, Kulite XCQ-80-100 transducers were employed, connected to a National Instruments USB-6356 data acquisition system operating at a 1 MHz sampling rate.

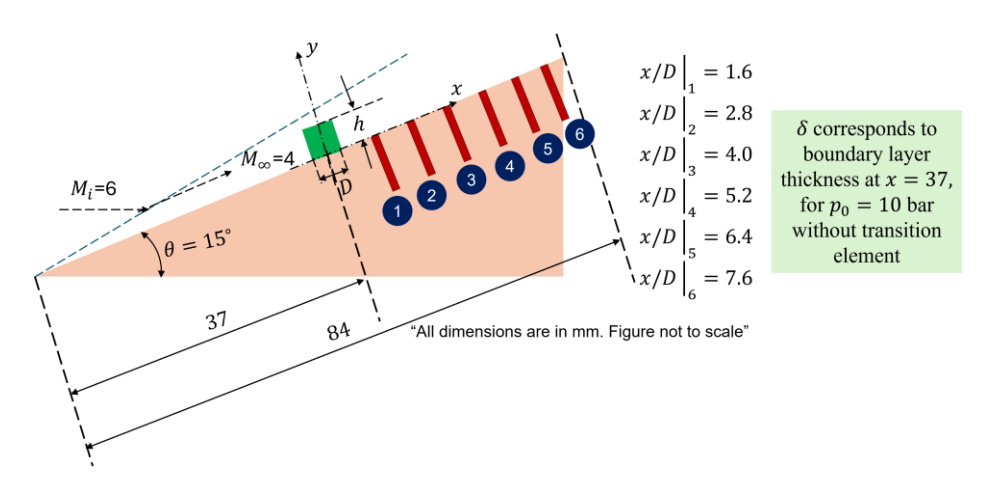


Fig.1 Wedge model used for present experiments.

Table 1. Flow Properties downstream of the leading edge.

Flow Properties (bar)	$p_0 = 4$	$p_0 = 6$	$p_0 = 8$	$p_0 = 10$
Mach Number (M_{∞})	4			
Free stream Reynolds number ($Re_{\infty} \times 10^6$, $1/m$)	8.8	13.2	17.1	21.6
Free stream pressure (p_{∞}, Pa)	1250.2	1846.4	2492.7	3127.3
Free stream temperature (T_{∞}, K)	71.64			
Free stream velocity $(u_{\infty}, m/s)$	677.12			
Free stream density (ρ_{∞} , kg/m^3)	0.061	0.089	0.1209	0.1520

3. Results

Figure 2 presents instantaneous Schlieren images obtained at Reynolds numbers of $8.8\times10^6\,\mathrm{m}^{-1}$ and $21.51\times10^6\,\mathrm{m}^{-1}$ for all roughness heights. The images indicate that the introduction of roughness elements disturbs the boundary layer downstream of the cylinder, leading to its thickening. At the lower Reynolds number $(8.8\times10^6\,\mathrm{m}^{-1})$, no significant flow modification is observed across the tested h/ δ configurations. In contrast, at the higher Reynolds number $(21.6\times10^6\,\mathrm{m}^{-1})$, the visualisations clearly show boundary layer thickening downstream of the roughness elements. As h/ δ increases from 0.46 to 1.15, the degree of thickening also increases. For h/ δ = 1.15, the most pronounced boundary layer growth is observed, accompanied by the appearance of vortical structures.

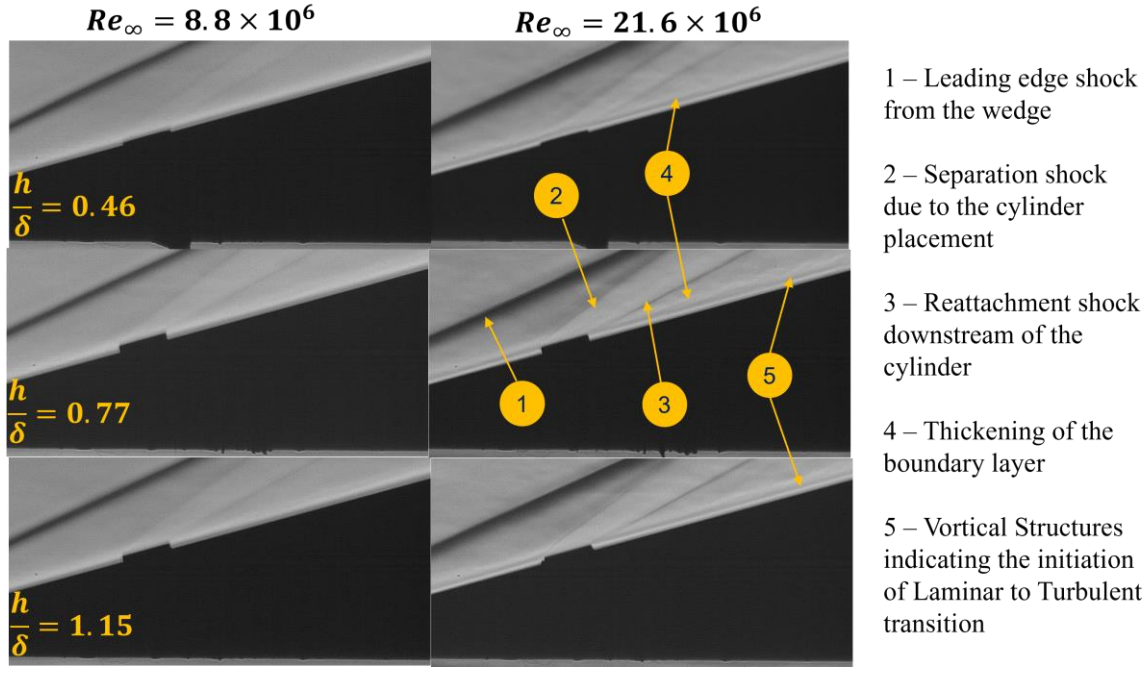


Fig.2 Schlieren Flow Visualization for the $h/\delta = 0.46, 0.77$ and 1.15.

Planar Laser Rayleigh Scattering (PLRS) is a non-intrusive optical diagnostic technique commonly used for quantitative measurement of gas density fields. The method relies on the principle that gas molecules elastically scatter incident light (Rayleigh scattering) when illuminated by a planar laser sheet (Nd: YAG laser at 532 nm). In PLRS, the flow field is visualized by recording the intensity of the scattered light from CO2 icicles, which is directly proportional to the local molecular density. Regions with high molecular concentration produce stronger scattered signals and appear as bright, high-gray-scale areas, whereas regions of reduced density—such as those with fewer CO2 molecules—appear darker with lower gray-scale intensity. Figure 3 presents instantaneous images obtained from Planar Laser Rayleigh Scattering (PLRS) at Re =21.51×10⁶m⁻¹ for h/ δ = 1.15. For a roughness height of h/ δ = 1.15, the PLRS image (Fig. 3) shows that the transition region begins at approximately x/D=2.5, coinciding with the development of shear instability. As unsteady fluctuations grow, a sequence of oblique vortical structures is shed from the shear layer, eventually breaking down into turbulence near the exit. The PLRS result clearly shows the formation of an array of vortical structures, indicating the onset of laminar-to-turbulent transition for h/ δ = 1.15.

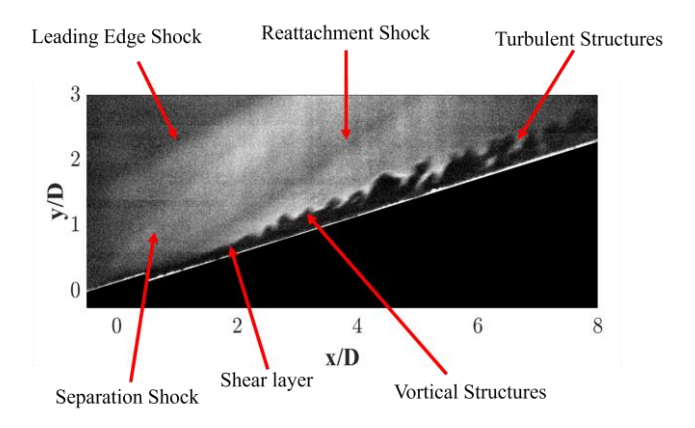


Fig.3 Instantaneous image of PLRS for $h/\delta = 1.15$ at $Re_{\infty} = 21.6 \times 10^6$.

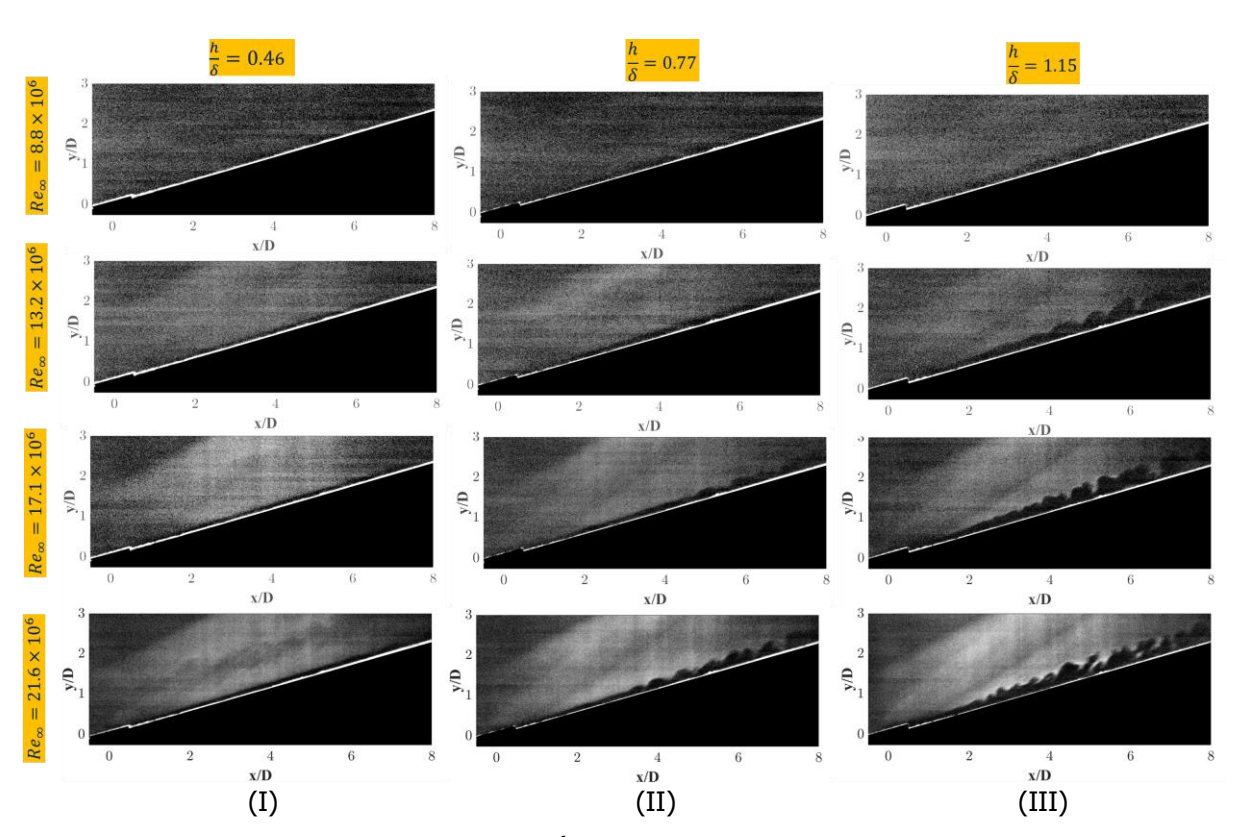


Fig.4 Instantaneous images of PLRS for $\frac{h}{\delta} = 0.46, 0.77$ and 1.15 for various Reynolds numbers.

Figure 4 presents instantaneous PLRS images acquired along the model centerline for all roughness configurations. For the case with $h/\delta=0.46$ (Fig. 4(I)), only minor modifications to the flow field are observed downstream of the roughness element. At the higher Reynolds number of 21.6×10⁶ m⁻¹, the boundary layer exhibits a slightly wavy structure near the model exit, though no distinct transition is evident. When the roughness ratio is increased to $h/\delta=0.77$ (Fig. 4(II)), the lower Reynolds number case (8.8×10⁶ m⁻¹) again shows only mild waviness in the boundary layer. However, as the Reynolds number is increased to $21.6 \times 10^6 \, \text{m}^{-1}$, a clear transition to turbulence is observed. For the largest roughness element, $h/\delta=1.15$, even at the lower Reynolds number of 8.8×10^6 m⁻¹, a noticeable increase in boundary layer thickness is evident compared to the cases having smaller step heights. At higher Reynolds numbers, the onset of transition is initiated, and by 21.6×10⁶ m⁻¹, the boundary layer exhibits fully developed turbulence.

HiSST-2025-274 7 | 4 Talluri Vamsi Krishna, Jacob Cohen and Soumya R. Nanda Copyright © 2025 by author(s)

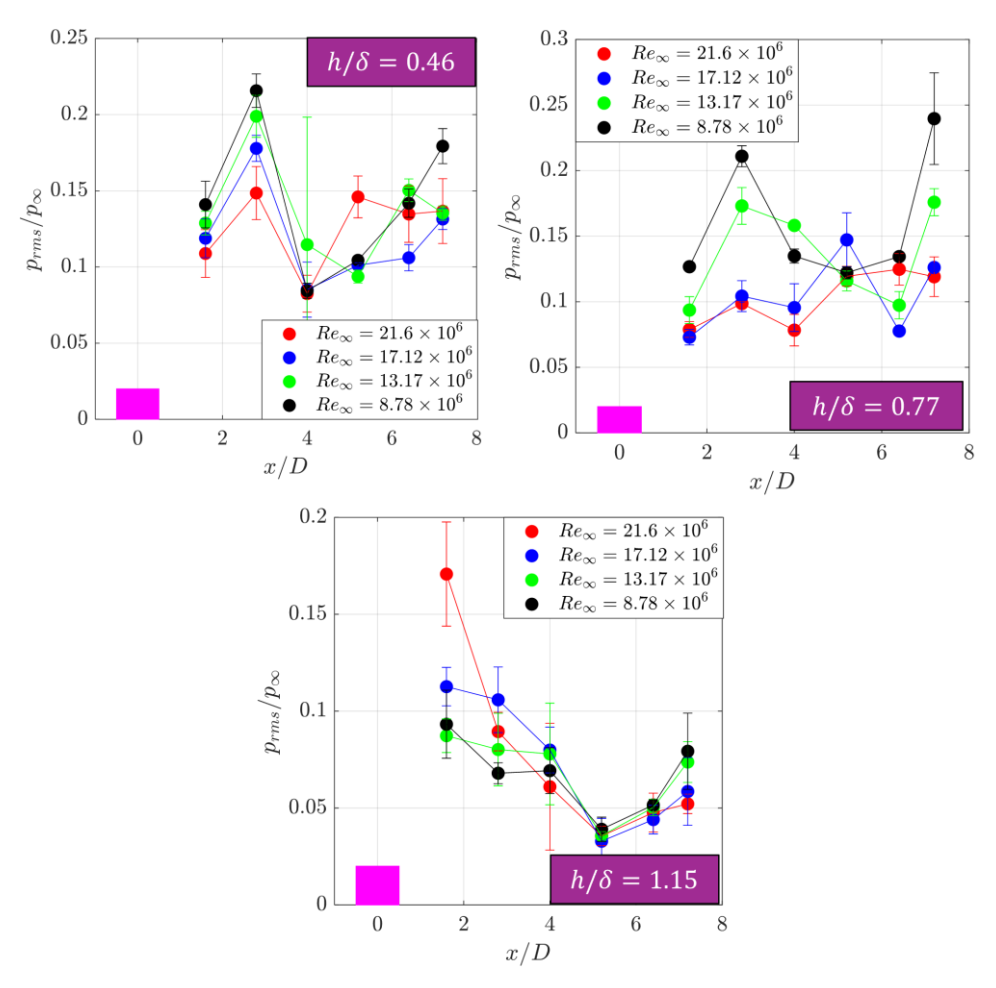


Fig.5 Normalized wall RMS pressure measured along the centerline of the model for the $h/\delta = 0.46, 0.77$ and 1.15 for all the Reynolds numbers.

Figure 5 presents the normalized root-mean-square (RMS) pressure variations for all investigated cases. The results for the $h/\delta=0.46$ configuration are shown in Figure 5a. As the flow progresses from x/D = 1.6 to 7.2, the RMS pressure initially increases, then undergoes a reduction, before rising again further downstream. The initial increase can be associated with shock impingement linked to flow reattachment or the near-wake region behind the cylinder. The subsequent decrease reflects pressure recovery toward ambient conditions, while the gradual rise further downstream suggests the possible onset of boundary-layer transition. This trend is consistent with the flow features identified in the Schlieren and PLRS visualizations discussed earlier for the same configuration. Figure 5b illustrates the RMS pressure distribution for the $h/\delta=0.76$ configuration. A similar trend to that of $h/\delta=0.46$ is observed in the near field. However, beyond x/D>5, the RMS pressure exhibits a more pronounced increase, indicating an earlier or more distinct onset of transition to turbulence. For the $h/\delta=1.15$ configuration (Figure 5c), the RMS pressure rises sharply just downstream of the cylindrical roughness element as a result of the strong wake it produces. With increasing x/D, the RMS pressure gradually decreases, followed by a secondary rise that signifies the transition of the boundary layer to turbulence. This behavior is consistently observed across all Reynolds numbers examined in this study.

To investigate the development of vortical structures, high-speed PLRS measurements were performed at 550 kfps with a spatial resolution of 128×64 pixels. Proper Orthogonal Decomposition (POD) was applied to the PLRS datasets for all the configurations. For the h/ δ =0.46 case, POD results at low Reynolds numbers revealed no dominant flow features. As the Reynolds number increased, a distinct dominant mode emerged, with coherent flow structures becoming apparent beyond x/D>5.0. The corresponding spectral analysis indicated a dominant frequency \sim 120 kHz.

In contrast, for the largest roughness element (h/ δ =1.15), the POD results shown in the right column of Figure 6 demonstrate that boundary layer transition initiates much earlier, beginning at approximately x/D=3.5 for Re $_{\infty}$ =21.6×10 6 m $^{-1}$. This transition is characterized by the appearance of alternating compression and rarefaction vortices. Spectral analysis across all configurations consistently identified a dominant mode, approximately 120 kHz. The spectra revealed distinct frequency bands may be associated with convective vortical structures, while similar kind dominant spectral content was observed in the literature was associated with first mode. Further analysis is needed to characterise the dominant mode.

Overall, the results indicate that increasing roughness height shifts the onset of transition upstream, while a similar upstream shift is also observed with increasing Reynolds number. These trends confirm that both larger roughness elements and higher Reynolds numbers promote earlier laminar-to-turbulent transition in hypersonic boundary layers.

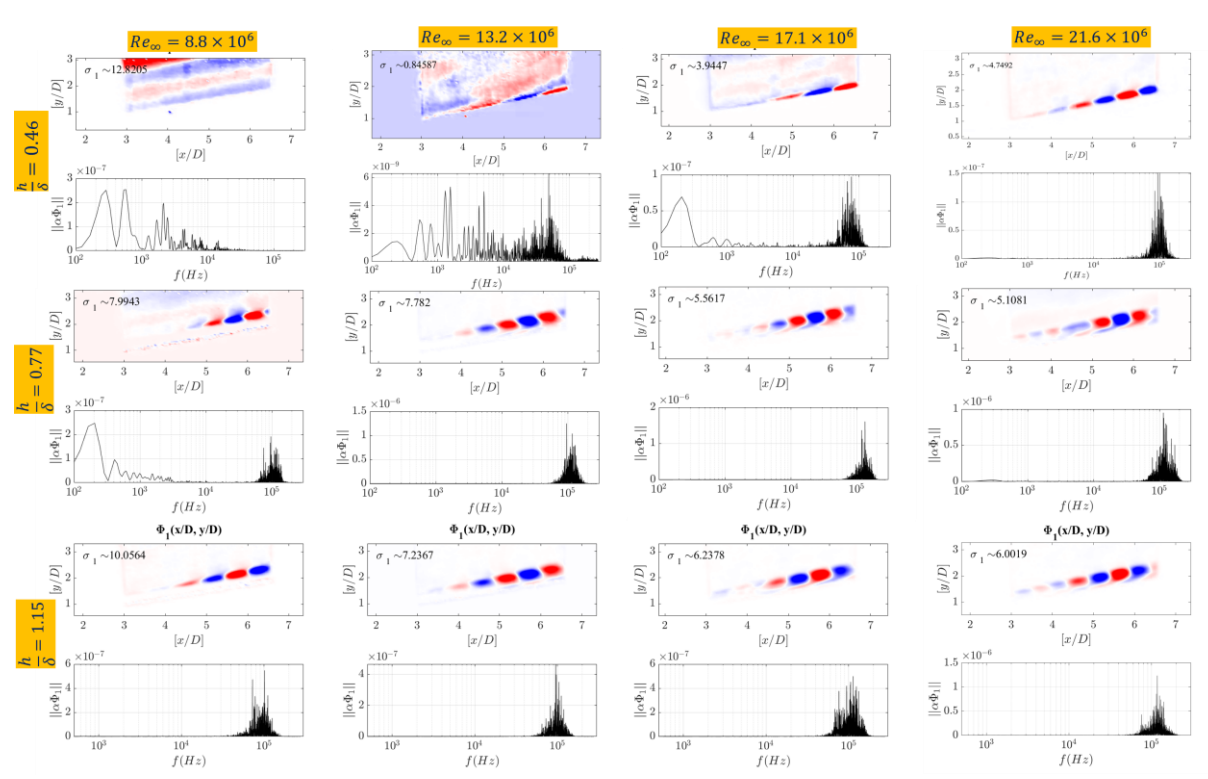


Fig.6 Proper orthogonal decomposition for h/δ values of 0.46, 0.77 and 1.15 across all Reynolds numbers.

4. Conclusion

An experimental investigation was carried out to study induced transition using cylindrical roughness elements with height-to-boundary-layer-thickness ratios of $h/\delta = 0.46$, 0.76, and 1.15. The experiments were conducted over a two-dimensional wedge model at hypersonic speeds across a range of Reynolds numbers. The key findings are as follows:

- Transition to turbulence was clearly observed for $h/\delta = 0.76$ and 1.15, while the $h/\delta = 0.46$ case largely remained laminar or at the onset of transition within the Reynolds numbers tested.
- RMS pressure measurements indicated that the initiation of transition shifted upstream with increasing Re $_{\infty}$ and with higher roughness ratios (h/ δ).
- Spectral analysis revealed that a distinct frequency band is associated with the initiation of the transition process.

HiSST-2025-274 7 | 6 *Talluri Vamsi Krishna, Jacob Cohen and Soumya R. Nanda* Copyright © 2025 by author(s)

• POD analysis clearly shows, the transition behavior was strongly dependent on roughness height, with the $h/\delta = 0.76$ and 1.15 configurations displaying clear turbulent signatures beyond x/D > 3.5, in contrast to the lower roughness case.

5. References

- 1. Mack, L. M.: Boundary-layer linear stability theory, Agard rep, vol. 709, 1984.
- 2. Arnal, D.: and Casalis, G.: Laminar-turbulent transition prediction in three-dimensional flows, Progress in Aerospace Sciences, vol. 36, no. 2, pp. 173–191, 2000.
- 3. Schneider, S. P.: Hypersonic laminar–turbulent transition on circular cones and scramjet forebodies, Progress in Aerospace Sciences, vol. 40, no. 1-2, pp. 1–50, 2004.
- 4. Dong, S., Chen, J., Yuan, X., Chen, X., and Xu, G.: Wall pressure beneath a transitional hypersonic boundary layer over an inclined straight circular cone, Advances in Aerodynamics, vol. 2, pp. 1–20, 2020.
- 5. Whitehead, A. H.: Flow-field and drag characteristics of several boundary-layer tripping elements in hypersonic flow, vol. 5454. National Aeronautics and Space Administration, 1969.
- 6. Karthick, S.K., Nanda, S. R., and Cohen, J.: Unsteadiness in hypersonic leading-edge separation, Experiments in Fluids, vol. 64, no. 1, p. 13, 2023.